Mem. S.A.It. Vol. 7, 114

Memorie della
Supplementi

A new approach for the structure of Hα regions in 120 Be-type stars

E. Lyratzi[1], E. Danezis[1], D. Nikolaidis[1], L. Č. Popović[2], M. S. Dimitrijević[2], E. Theodossiou[1] and A. Antoniou[1]

[1] University of Athens, School of Physics, Department of Astrophysics, Astronomy and Mechanics, Panepistimiopolis, Zografos 157 84, Athens - Greece
[2] Astronomical Observatory, Volgina 7, 11160 Belgrade, Serbia
e-mail: elyran@cc.uoa.gr

Abstract. The spectra of most Oe and Be stars present Discrete or Satellite Absorption Components (DACs or SACs respectively) which result to complex structure of line profiles of these stars. The DACs are spectral lines of the same ion and the same wavelength as a main spectral line, shifted at different $\Delta\lambda$, as they are created from different density regions, which rotate and move radially with different velocities. However, if the regions, which give rise to such lines rotate with large velocities and move radially with small velocities, the produced lines are much broadened and little shifted. As a result they are blended among themselves as well as with the main spectral line and thus they are not discrete. In such a case the name Discrete Absorption Component is inappropriate and we use only the name SACs (Satellite Absorption Components). In this paper we present a statistical study of the Hα line profiles of 120 Be-type stars using the model proposed by Danezis et al. (2003); Lyratzi & Danezis (2004). This model proposes that the density layers which produce the Hα line lie in different regions in the stellar atmosphere. In the Be-type stellar atmospheres, there are two regions that can produce the Hα satellite components. The first one lies in the chromosphere and the second one in the cool extended envelope. We concluded that the chromospheric components are best reproduced by the proposed Rotation distribution (Danezis et al. 2003; Lyratzi & Danezis 2004). The absorption components which are created in the cool extended envelope are best reproduced by a Gaussian distribution. The emission components, if they exist, they are best reproduced by a Voigt distribution. By fitting the Hα line profiles with the line function of the proposed model we are able to calculate: a) For the chromospheric absorption components we calculated the rotational and radial velocities as well as the optical depth. b) For the emission and absorption components which are created in the cool extended envelope we calculated the radial velocities, the FWHM and the optical depth. Finally, we present the relation between these parameters with the spectral subtype and the luminosity class.

Key words. Stars: early type – Stars: atmospheres – Stars: Hα

1. Introduction

The Hα line's profile is the most often and mostly studied profile in the spectra of early type stars. Andrillat & Fehrenbach (1982); Andrillat (1983) observed that the structure of the emission of Ha line appears to be both very complex and variable and, in most cases, a central absorption is present. In some spectra, the stellar absorption (called "photospheric line") is present and the emission line, having, probably, chromospheric origin, is superposed on it. Hutchings (1971) proposed that the changes in the profiles may be attributed to the rotation of the stars together with inhomogeneities in their envelopes. These phenomena could result from the existence of "knots" of higher-density material in the extended equatorial envelope, which are released at the photosphere (Hutchings 1970a,b; Bohlin 1970). (Slettebak & Reynolds 1978) proposed that the changes of the shape and the total energy in the Hα emission line profile of a Be-type star could result from motions within the shell surrounding the star, from a change in the amount of emitting material in the shell, or both. Doazan (1970) observed that for the 26 studied Be-type stars, the velocities extracted from the width of the emission lines of Ha, are greater than the rotational velocity ($V sini$) of the central star. She proposed that the great width of the emission lines of H is due to the motion of the envelope, as well as to the motion of matter which is placed in regions far from the central star. She pointed out that the rotation does not provide enough arguments to explain the observed widths of the emission lines. In order to explain the large observed Ha emission-line half-width, another source of line broadening is required in addition to envelope rotation, such as electron scattering (Poeckert & Marlborough 1979; Dachs et al. 1981). Andrillat & Fehrenbach (1982); Andrillat (1983) accept that this phenomenon is due to electron scattering (Marlborough 1969), or due to the envelope rotation as well as to the motion of the material inside the envelope (Gray & Marlborough 1974; Poeckert & Marlborough 1979).

Send offprint requests to: E. Lyratzi

In this paper, by applying the model proposed by Danezis et al. (2003); Lyratzi & Danezis (2004), we study whether the hypothesis of Discrete Absorption Components (DACs) and Satellite Absorption Components (SACs) is able to explain the complex structure of Hα lines' profile of 120 Be-type stars. With this method we calculate some physical parameters, such as the rotational (V_{rot}) and radial velocities (V_{rad}), as well as the full width at half maximum (FWHM) and the optical depth (ξ), of the independent density layers of matter in the atmospherical regions, where the Hα line is created.

2. Description of the model

We consider that:

- The atmospherical region where a specific line is created is not continuous, but it is composed of a number of successive independent absorbing density regions, a number of emission regions and an external general absorption region.
- The angular velocity of rotation is constant.
- None of the phenomena is relativistic.
- The only effect of a shell's expansion or contraction is a Doppler shift from the laboratory wavelength.

By solving the equations of radiation transfer through a complex structure as the one described, we conclude to the following function for the line's profile:

$$I_\lambda = \left[I_{\lambda 0} \prod_i e^{-x_i} + \sum_j S_{\lambda ej} \left(1 - e^{-x_j}\right) \right] e^{-x_g} \quad (1)$$

where:

$I_{\lambda 0}$: is the initial radiation intensity,

$S_{\lambda ej}$: is the source function, which, at the moment when the spectrum is taken, is constant and

e^{-x} : is the appropriate distribution function (Gauss, Lorentz, Voigt, Rotation)

The function (1) is able to give the best fit for the main spectral line and its Satellite Absorption Components in the same time. Such a best fit, through the function of the line's profile, enables us to calculate some parameters (rotational and radial velocities, FWHM, optical depth) of the independent layers of matter, which form the main spectral line and its satellite absorption components.

2.1. The Rotation distribution function

We consider that the density regions, where the SACs or DACs are created, present spherical symmetry and that the main reason of the spectral lines' broadening is the rotation of the density regions which create them and we calculated the Rotation distribution function $e^{-L\xi}$, where:

ξ is the optical depth in the center of the spectral line and

$$L(\lambda) = \begin{cases} \sqrt{1-\cos^2\theta_0}, \text{if} \cos\theta_0 < 1 \\ 0, \text{if} \cos\theta_0 \geq 1 \end{cases}$$

where:

$$\cos\theta_0 = \frac{-\lambda_0 + \sqrt{\lambda_0^2 + 4\Delta\lambda_{rotation}^2}}{2\Delta\lambda_{rotation} z_0}$$

λ_0 is the observed wavelength of the center of the spectral line,

$\Delta\lambda_{rotation}$ is the broadening of the spectral line and

$z_0 = \frac{\Delta\lambda_{rotation}}{\lambda_{lab}} = \frac{V_{rotation}}{c}$, where λ_{lab} is the laboratory wavelength of the spectral line.

In case we do not want to consider certain geometry, but only some physical parameters, we may replace the Rotation distribution function ($e^{-L\xi}$) with a classical distribution function (Gauss, Lorentz, Voigt). This means that when we consider that the lines' broadening is mainly due to the ions' random motion, we apply a Gaussian distribution and when we consider that the lines' broadening is mainly due to the collisional effects among the ions we apply a Lorentzian distribution. Finally, if the lines' broadening is due to the ions' random motion, as well as the collisional effects among the ions, which, in an environment of high pressure and temperature, result to the broadening of the produced spectral lines, we apply the Voigt distribution function (synthesis of a Gaussian and a Lorentzian distribution).

3. Application of the model to the Hα line of 120 Be-type stars

In our study we use the stellar spectrographs of 120 Be-type stars, which were taken by Andrillat & Fehrenbach (1982); Andrillat (1983) (resolution 5,5 and 27 Å) with the telescope of 152 *cm* in the Observatory of Haute Provence. In Table 1 we give the list of stars and their spectral type.

4. Results

In most of the Be stellar spectra the Hα line presents peculiar and complex profiles. Usually the Hα line's profile consists of a very broad absorption component, an emission component and a narrow absorption component.

We applied the proposed model, in order to reproduce the complex profiles of the Hα line 6562.817 Å in the spectra of the 120 studied Be-type stars of all the spectral subtypes and luminosity classes. We tried to fit the observed profiles by applying all the classical distributions (Gauss, Lorentz, Voigt, Rotation).

We concluded that the best fit is accomplished when we fit the very broad absorption line with Rotation distribution (the broad absorption line is composed by one to five satellite absorption components), the emission component with Voigt distribution (in 7 of the 120 stars there exist two emission components) and the narrow absorption component with Gauss distribution.

The most important point is that the best fit is not a graphical composition of the distributions for each component, but it is the result of the final function (function 1) of the model, where the appropriate distribution is applied in the place of the exponential e^{-x}. In Fig. 1 we present the best fit of two of the studied stars, as well as all the components to which the observed profile is analyzed by the model.

In the following diagrams the points correspond to the mean values of the calculated parameters, extracted for each spectral subtype or luminosity class and the error bars, which appear in some of the diagrams, correspond not

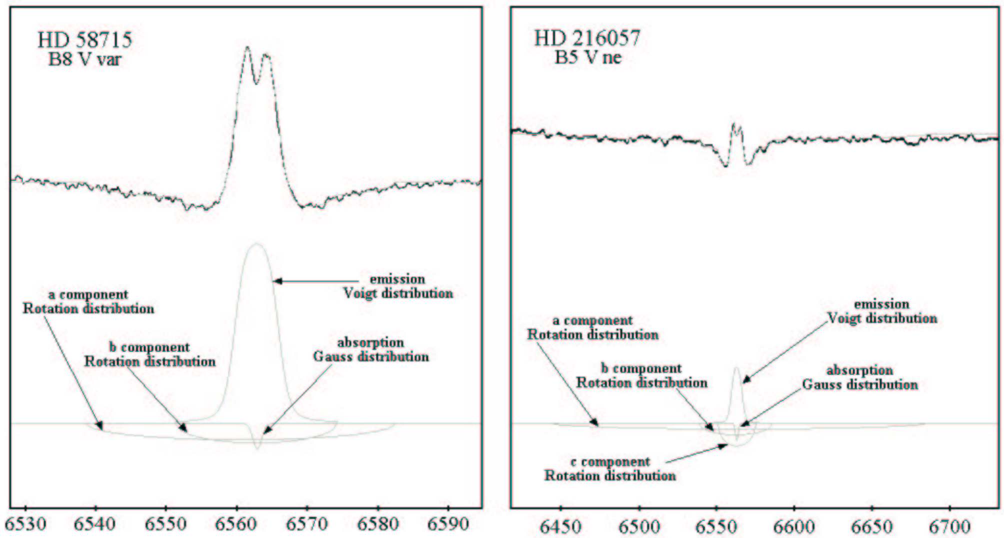

Fig. 1. Best fit of the Hα line profiles of the Be-type stars HD 58715 and HD 216057. The black lines present observations, and the gray lines the best fit. The SACs are present below.

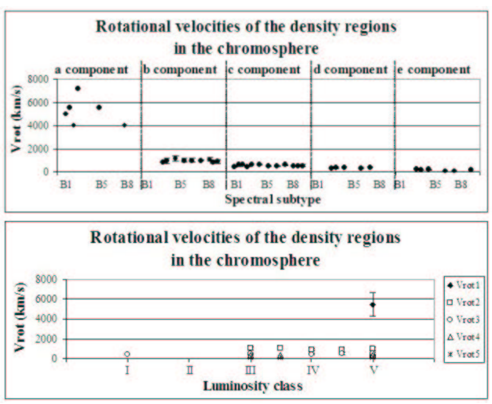

Fig. 2. Mean values of the rotational velocities, as a function of the spectral subtype and the luminosity class, for the five density regions in the chromosphere. The rotational velocities of the five density regions are 5200±1192 km s^{-1}, 990±170 km s^{-1}, 536±68 km s^{-1}, 352±37 km s^{-1} and 152±46 km s^{-1}. The dispersion of the values around the respective mean value, decreases from the first to the fifth density region. The very broad components (large rotational velocities) are present in the spectra of dwarfs.

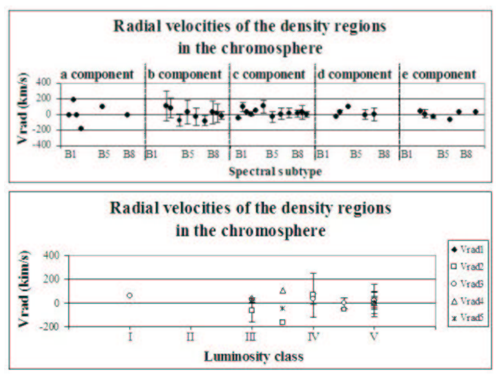

Fig. 3. Mean values of the radial velocities, as a function of the spectral subtype and the luminosity class, of the five density regions in the chromosphere. The five density regions move radially with velocities 15±121 km s^{-1}, 7±123 km s^{-1}, 19±62 km s^{-1}, 15±60 km s^{-1} and -2±42 km s^{-1}.

only to the statistical errors but also to the dispersion around the mean values.

5. Conclusions

We applied the proposed model on the Hα line's profiles of 120 Be-type stars in order to investigate the kinematical properties of the Hα line forming region. We obtained the rotational and radial velocities, the FWHM and the optical depth, which allow us to extract some

Table 1. The list of Be-type stars with spectral type

Star	Spectral Type	Star	Spectral Type	Star	Spectral Type
HD 5394	B0 IV evar	HD 32343	B2.5 V e	HD 109387	B6 III pe
HD 53367	B0 IV e	HD 37967	B2.5 V e	HD 224544	B6 IV e
HD 34921	B0 IV pe	HD 65875	B2.5 V e	HD 23480	B6 IV e
HD 203374	B0 IV pe	HD 187811	B2.5 V e	HD 37330	B6 V
HD 206773	B0 IV pe	HD 191610	B2.5 V e	HD 43285	B6 V e
HD 33152	B1 V e	HD 208682	B2.5 V e	HD 217891	B6 V e
HD 200310	B1 V e	HD 20336	B2.5 V ne	HD 138749	B6 V nne
HD 212571	B1 V e	HD 60855	B2/B3 V	HD 23630	B7 III
HD 19243	B1 V e	HD 51345	B3 ne	HD 196712	B7 III ne
HD 35439	B1 V pe	HD 37490	B3 III e	HD 209409	B7 IV e
HD 38010	B1 V pe	HD 50083	B3 IV e	HD 6811	B7 V e
HD 44458	B1 V pe	HD 189687	B3 IV e	HD 192044	B7 V e
HD 207329	B1.5 Ib e	HD 203467	B3 IV e	HD 22780	B7 V ne
HD 24560	B1.5 V nne	HD 50820	B3 IV e	HD 210129	B7 V ne
HD 200120	B1.5 V ne	HD 45725	B3 V e	HD 20566	B8
HD 193237	B2 pe	HD 25940	B3 V e	HD 26398	B8
HD 203025	B2 III e	HD 40978	B3 V e	HD 6343	B8
HD 45910	B2 III e	HD 45725	B3 V e	HD 81357	B8
HD 37202	B2 IV p	HD 183362	B3 V e	HD 142983	B8 Ia/Iab
HD 199356	B2 IV p	HD 208057	B3 V e	HD 174638	B8 II
HD 36576	B2 IV/V e	HD 37657	B3 V e	HD 50658	B8 III e
HD 197419	B2 IV/V e	HD 205637	B3 V p	HD 193911	B8 III ne
HD 212076	B2 IV/V e	HD 217543	B3 V pe	HD 29866	B8 IV ne
HD 30076	B2 V e	HD 217050	B4 III pe	HD 23862	B8 nn
HD 32991	B2 V e	HD 71072	B4 III/IV	HD 47054	B8 V e
HD 58050	B2 V e	HD 201733	B4 IV pe	HD 58715	B8 V var
HD 164284	B2 V e	HD 44996	B4 V	HD 183914	B8 V ne
HD 202904	B2 V e	HD 175863	B4 V e	HD 18552	B8 V ne
HD 11606	B2 V ne	HD 55135	B4 V ne	HD 23552	B8 V ne
HD 41335	B2 V ne	HD 224559	B4 V ne	HD 185037	B8 V ne
HD 52721	B2 V ne	HD 33988	B5	HD 199218	B8 V nne
HD 58343	B2 V ne	HD 21650	B5	HD 61224	B8/B9 IV
HD 148184	B2 V ne	HD 205060	B5	HD 91120	B8/B9 IV/V
HD 194335	B2 V ne	HD 89884	B5 III	HD 9709	B9
HD 65079	B2 V ne	HD 4180	B5 III e	HD 50138	B9
HD 28497	B2 V ne	HD 22192	B5 V e	HD 207232	B9
HD 45995	B2 V nne	HD 171780	B5 V ne	HD 62367	B9
HD 10516	B2 V pe	HD 216057	B5 V ne	HD 142926	B9 pe
HD 187567	B2.5 IV e	HD 23302	B6 III e	HD 144	B9 III e
HD 203699	B2.5 IV ne	HD 45542	B6 III e	HD 195554	B9 V e

general physical properties for the Hα regions of Be-type stars. Some interesting results inferred from the investigations are the following:

1. The proposed line function (function 1) is able to reproduce accurately the complex profiles of all the 120 studied Be-type stars. This means that the regions where the Hα line is created are not continuous, but they

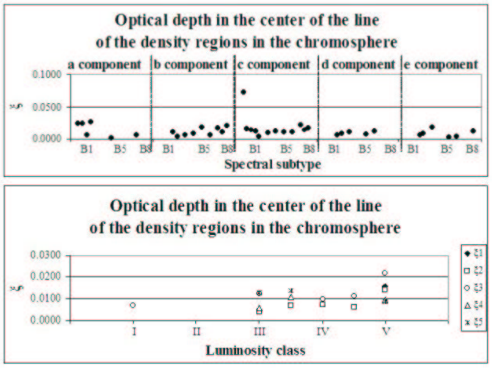

Fig. 4. Mean values of the optical depth in the center of the line, as a function of the spectral subtype and the luminosity class, for the five density regions in the chromosphere. The optical depth ξ in the center of the line, for the five density regions, lies between the values a) 0.0020 and 0.0255, b) 0.0033 and 0.0964, c) 0.0029 and 0.1296, d) 0.0024 and 0.0196 and e) 0.0025 and 0.0230.

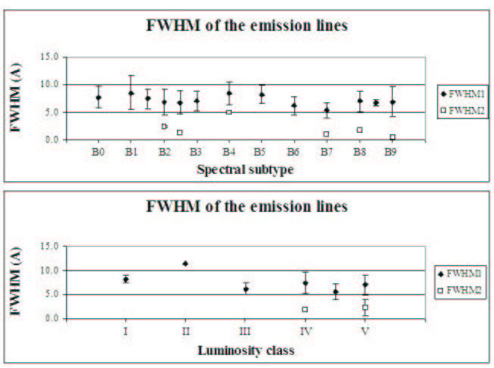

Fig. 5. Mean values of the FWHM of the emission components, as a function of the spectral subtype and the luminosity class. For the main emission component, the FWHM fluctuates around the value of 7.1 Å. For the second emission component (where it appears) the fluctuation of the FWHM is around the value of 2.0 Å.

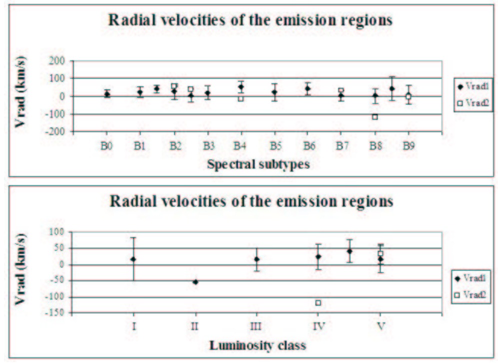

Fig. 6. Mean values of the radial velocities of the emission components, as a function of the spectral subtype and the luminosity class. The radial velocity of the two components fluctuates around the value of 20 km s^{-1}.

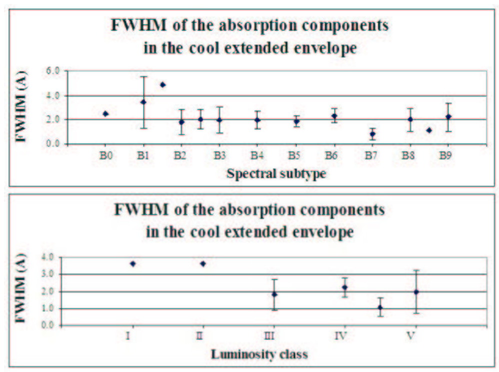

Fig. 7. Mean values of the FWHM of the absorption component which is created in the cool extended envelope, as a function of the spectral subtype and the luminosity class. The FWHM fluctuates around the value of 2.0 Å.

consist of successive independent density regions. In the place of the exponential e^{-x}, which gives the profile of each component, we apply the appropriate distribution function. The choice of the appropriate distribution function depends on the physical conditions of the regions which create the SACs. The most important point is that, in any case, the proposed line function remains the same. The important advantage of this method is that we are able to accomplish the best fit of the observed spectral lines, by applying a line function, to which we conclude after the solution of the radiation transfer equations, through a complex atmospherical structure, and not by a graphical composition of mathematical distribution functions with no physical meaning.

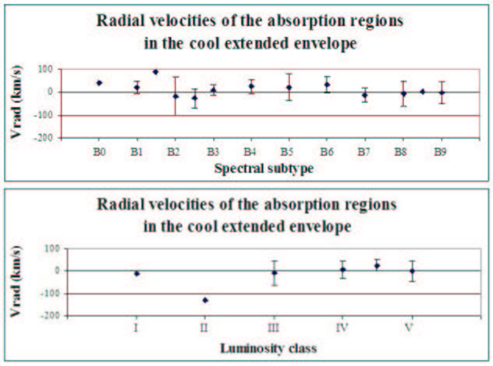

Fig. 8. Mean values of the radial velocity of the absorption component which is created in the cool extended envelope, as a function of the spectral subtype and the luminosity class. The radial velocity fluctuates around the value of 0 km s^{-1}.

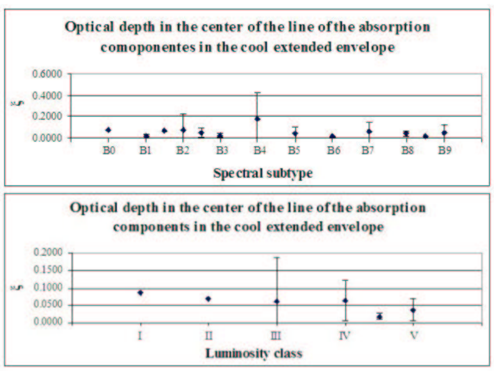

Fig. 9. Mean values of the optical depth in the center of the line of the absorption component which is created in the cool extended envelope, as a function of the spectral subtype and the luminosity class. The optical depth ξ in the center of the line lies between the values 0.0039 and 0.6250.

2. The existence of SACs is a general phenomenon in the spectra of Be-type stars. The profiles of the studied spectral lines appear to be peculiar and complex, as they do not present only one spectral line, but a number of SACs, which are created in independent density regions. In most cases, the observed profiles of the Hα line consist of, at most, five broad absorption components, an emission component (in 7 of the 120 studied stars there is also a second emission component) and a narrow absorption component.
3. The atmospheric region which creates the broad absorption components lies in the cromosphere and consists of one to five successive independent density regions, which are spherically symmetric around the center of the star and rotate with different velocities. These regions do not appear in all the studied stars. Each one of these layers creates one independent broad satellite absorption component (SAC). As the Be-type stars are rapid rotators, the main reason of the broadening of these components is the rotation of the forming regions. The rotational velocities of these layers are 5200±1192 km s^{-1}, 990±170 km s^{-1}, 536±68 km s^{-1}, 352±37 km s^{-1} and 152±46 km s^{-1}. The radial velocity of all the regions presents dispersion around the value of 12 km s^{-1}. These density regions have different densities. The denser layers are the ones that rotate with middle velocities (between 400 and 1050 km s^{-1}). These dense layers are observed only in dwarfs and do not depend on the spectral subtype.
4. The emission components are created in density regions in the cool extended envelope. These regions lie in great distance from the star, meaning that their rotation cannot be the main reason of the broadening of the produced components. Their broadening results from the random motion of the ions as well as the collisional effects, which in an environment of great pressure and low temperature, result to the broadening of the produced components. The radial velocity of the emission regions is about 20 km s^{-1}. The FWHM of the emission components lies between the values of 2.3 and 12.3 Å. In few cases (7 of the 120 studied stars) a second emission region appears which moves radially with 6 km s^{-1} and creates emission components with FWHM between the values of 0.5 and 5.0 Å. The denser emission regions create relatively narrow components (FWHM between 3.3 and 8.1 Å), independently of the spectral subtype and the luminosity class.

5. The narrow absorption components are also created in density regions in the cool extended envelope. These regions lie in great distance from the star, meaning that their rotation cannot be the main reason of the broadening of the produced components. The main reason of their broadening is the random motion of the ions. The radial velocity of the narrow absorption regions is about 0 km s^{-1}. The FWHM of the narrow absorption components lies between the values of 0.3 and 5.6 Å. The denser narrow absorption regions create the most narrow components (FWHM between 1.3 and 3.3 Å), independently of the spectral subtype. These denser regions are observed mostly in the supergiants.

Acknowledgements. This research project is progressing at the University of Athens, Department of Astrophysics, Astronomy and Mechanics, under the financial support of the Special Account for Research Grants, which we thank very much. This work also was supported by Ministry of Science and Environment Protection of Serbia, through the projects P1195 (Influence of collisional processes on astrophysical plasma line shapes) and P1196 (Astrophysical spectroscopy of extragalactic objects).

References

Andrillat, Y., & Fehrenbach, Ch. 1982, A&AS, 48, 93
Andrillat, Y. 1983, A&AS, 53, 319
Bohlin, R. C. 1970, ApJ, 162, 571
Dachs, J., et al. 1981, A&AS, 43, 427
Danezis, E., et al. 2003, Ap&SS, 284, 1119
Doazan, V. 1970, A&A, 8, 148
Gray, D. F., & Marlborough, J. M. 1974, ApJS, 27, 121
Hutchings, J. B. 1971, MNRAS, 152, 109
Hutchings, J. B. 1970a, MNRAS, 147, 161
Hutchings, J. B. 1970b, MNRAS, 150, 55
Hutchings, J. B. 1971, MNRAS, 152, 109
Lyratzi, E., & Danezis, E. 2004, AIP Conference Proceedings 740, pp. 458-473 [THE PHYSICS OF IONIZED GASES: 22nd Summer School and International Symposium on the Physics of Ionized Gases, Bajina Bašta, 23-27 August 2004, eds. Lj. Hadzijevski, T. Grozdanov, N. Bibić]
Marlborough, J. M. 1969, ApJ, 156, 135
Poeckert, R., & Marlborough, J. M. 1979, ApJ, 233, 259
Slettebak, A., & Reynolds, R. C. 1978, ApJS, 38, 205